Supporting Information for

Tough and recyclable phase-separated supramolecular gels via a dehydration-hydration cycle

Xiaohui Xu[1], Yannick L. Eatmon[2], Kofi S.S. Christie[4,5], Allyson L. McGaughey[4,5], Néhémie Guillomaitre[1,2], Sujit S. Datta[1], Zhiyong Jason Ren[4,5], Craig Arnold[2], Rodney D. Priestley[1,3*]

[1]Department of Chemical and Biological Engineering, Princeton University, Princeton, New Jersey 08540, United States

[2]Department of Mechanical and Aerospace Engineering, Princeton University, Princeton, New Jersey 08540, United States

[3]Princeton Institute for the Science and Technology of Materials, Princeton University, Princeton, New Jersey 08540, United States

[4]Department of Civil and Environmental Engineering, Princeton University, Princeton, New Jersey 08540, United States

[5]Andlinger Center for Energy and the Environment, Princeton University, Princeton, New Jersey 08540, United States

*Corresponding author email: rpriestl@princeton.edu

Experimental Section

Materials: Sodium styrenesulfonate (NaSS), *N*,*N*′-methylenebisacrylamide (Bis), Irgacure 2959, poly(vinyl alcohol) (PVA, *Mn* 8900), , acrylamide, and sulfobetaine methacrylate (SBMA, 97%) were obtained from Sigma-Aldrich and used without further purification.

Recycling of PSG gels: The PSG hydrogel in a vial was placed in an oven at 90 °C for fast disassociation. The white PSG gel gradually melted with increasing heating time and formed a translucent, viscous solution. Then, the viscous solution was poured into different containers or molds, cooled at room temperature, and dehydrated in air. The dehydrated solid gel was then transferred into DI water for rehydration. In this way, new PSG samples with various shapes were obtained.

Measurement of antifouling performance: Fouling resistance was characterized using colloid probe force microscopy (MFP-3D, Asylum Research, Santa Barbara, CA, USA), similar to methods reported in the literature (e.g., Horseman et al.[1], Davenport et al.[2], Liu et al.[3,4]). Measurements were performed using a 5-μm diameter soft polyethylene colloidal probe (Novascan, Ames, IA, USA) as a model colloidal oil foulant, as in a previous study (i.e., Horseman et al.[1]). All measurements were performed in an aqueous solution of 50 mM NaCl and 0.5 mM $CaCl_2$, as in previous studies.[2-4] Samples were equilibrated in solution for at least 30 minutes before characterization. Four hundred individual force curves were obtained at separate locations within a 20 by 20 μm area near the center of the sample; force curves were analyzed using Igor Pro software (Asylum Research).

Materials Characterizations: The morphologies of freeze-dried gels were characterized by scanning electron microscopy (Verios 460 XHR SEM). Underwater oil contact angles were measured on an OCA20 machine (Data Physics). Surface morphology was characterized via atomic force microscopy (MFP-3D, Asylum Research); data were analyzed using Gwyddion software (version 2.60, Czech Metrology Institute, Brno, Czech Republic). Mechanical properties were investigated using an Instron with a 5 KN load cell. Hydrogels with cylindrical and dog-bone shapes were employed for the compression and tensile tests, respectively.

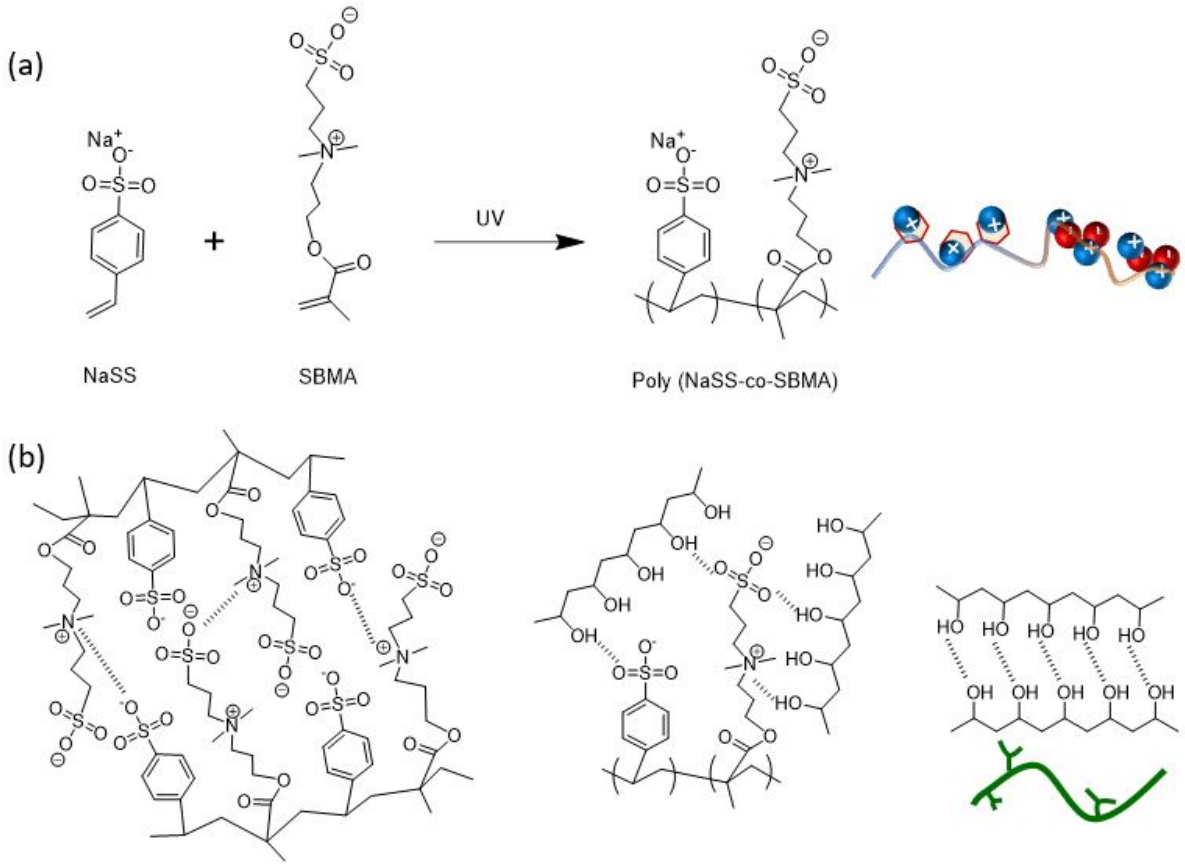

Fig. S1. (a) The chemical structures of the monomers and the poly(NaSS-*co*-SMBA) copolymer. (b) The polymer-polymer interactions in the PSG include the electrostatic interactions between the poly(NaSS-*co*-SMBA) copolymers, the hydrogen bonding between the copolymer and PVA, and the hydrogen bonding between PVA chains. The hydrophobic interactions between polymer backbones are not shown.

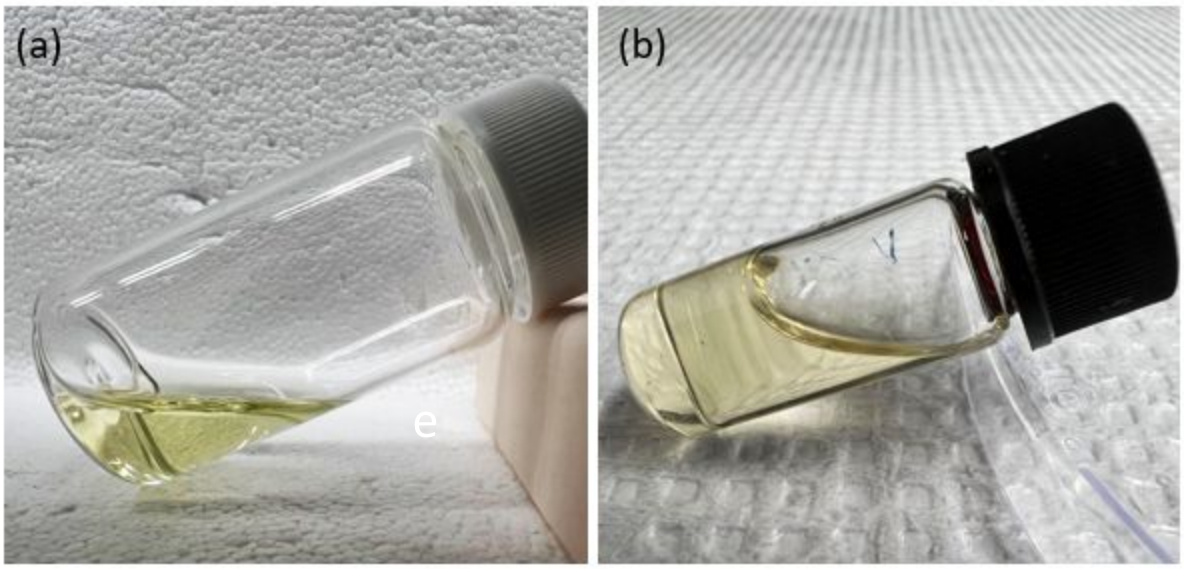

Fig. S2. (a) Polymerization of NaSS and SBMA in the absence of PVA. (b) Polymerization of SBMA in PVA solution in the absence of NaSS.

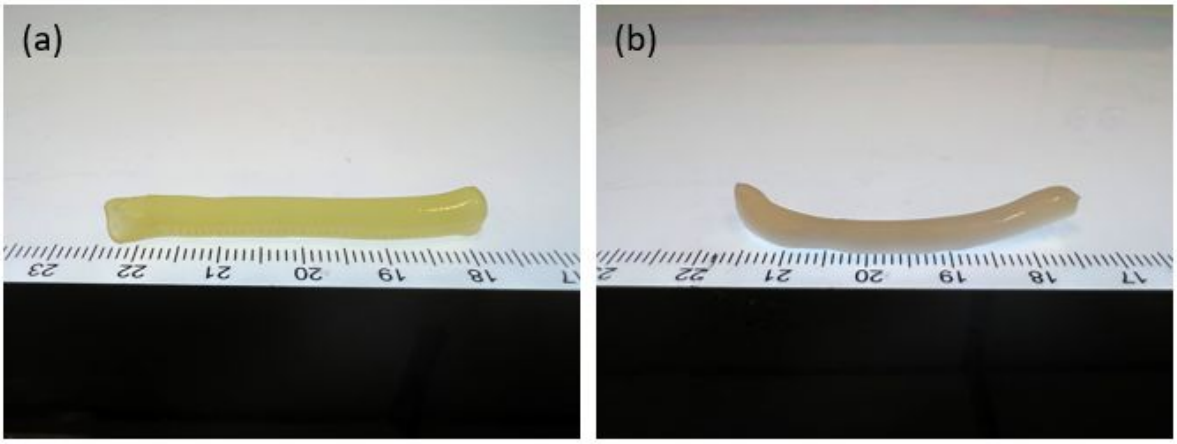

Fig. S3. Optical photos of (a) SG and (b) PSG

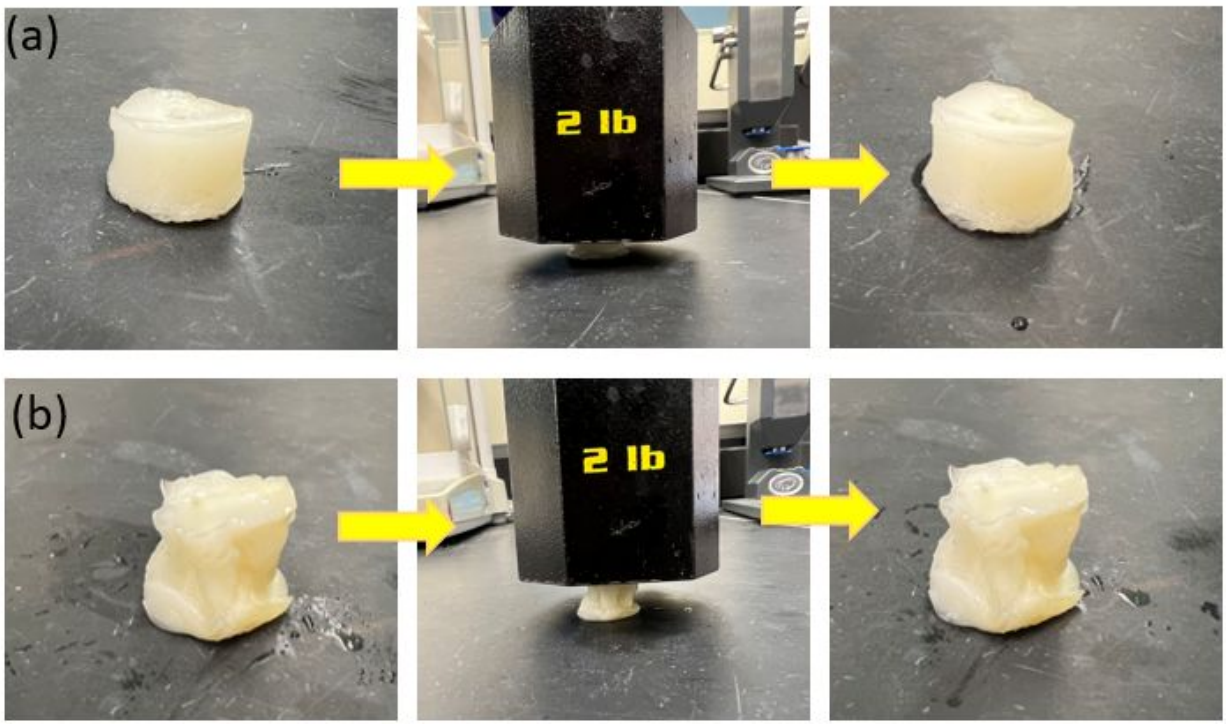

Fig. S4. (a) Polyacrylamide/PVA hydrogels and (b) Poly(N,N-dimethylacrylamide)/PVA hydrogels prepared via the dehydration-rehydration method.

We prepared polyacrylamide/PVA hydrogels and Poly(N,N-dimethylacrylamide)/PVA hydrogels using the dehydration-rehydration strategy to demonstrate the generality of this approach. As depicted in Fig. S4, the resulting gels displayed an opaque color, indicative of phase separation within the hydrogels. When subjected to a 2 lb weight load, the hydrogels showed no signs of fracturing or irreversible deformation. This is attributed to the formation of phase-separated hard domains, which act as physical crosslinks reinforcing the polymer network. the gels remain soft and are unable to retain their shape after being removed from the container (figure not shown).

The typical stress−strain curves of SG and PSG exhibited elastic behavior, which can be tailored by varying the molar ratios of the monomers during polymerization (**Fig. S5**). In comparison with the very soft SG, the PSG exhibited greater toughness. This indicates that the phase-separated hard domains in the PSG could form stable physical crosslinks within the hydrogels through the dehydration-rehydration process (**Fig. S5a, b**). Cyclic tensile tests of PSG were performed to evaluate the self-recoverability of the PSGs at a constant loading/unloading rate of 100 mm min^{-1}. **Fig. S5c** shows the single cyclic stress-strain curves of the PSG with a 50:50 monomer ratio at different strains (50%, 100%, 150%, 200%). It was observed that the PSG displayed a hysteresis loop at each tested strain, a key feature of high toughness. The hysteresis loop became more pronounced with increasing tensile strain. This result indicates that the PSG efficiently dissipated strain energy by breaking the dynamic hydrogen bonds during mechanical cycling. A typical compressive test was carried out by uniaxially compressing the specimen to 80% strain, and the corresponding stress–strain curves are shown in **Fig. S5d, e**. The SG and PSG exhibited the highest compressive strength of 0.3 MPa and 1.8 MPa with a 50:50 monomer ratio, respectively. After removing the external stress, the SG with varied monomer ratios stayed deformed with slight shape recovery (inset image in **Fig. S5d**).

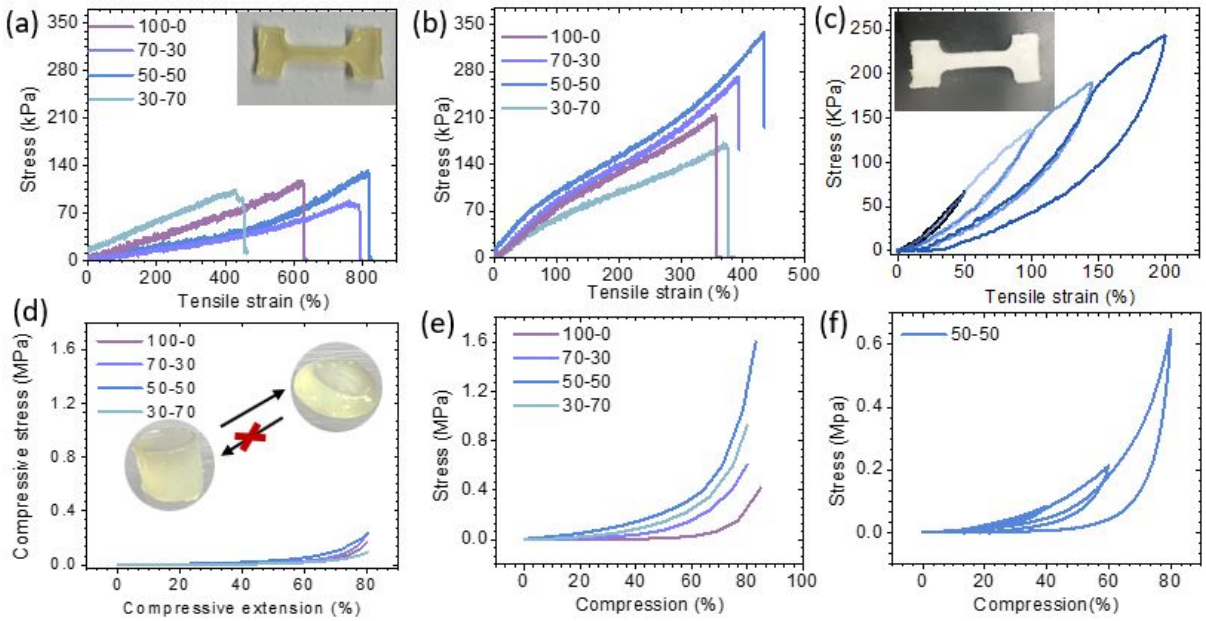

Fig. S5. Mechanical characterization of the hydrogels. Typical tensile stress-strain curves of (a) SG and (b) PSG with various monomer ratios. (c) Successive cyclic tensile behavior of PSG (with monomer ratio of 50:50) at varied strains (50%, 100%, 150%, 200%). Compressive stress–strain curves of the (d) SG and (e) PSG. (f) Cyclic compression behavior of PSG at varied strains (20%, 40%, 60%, 80%).

Under extreme compression (90 %), the PSG rapidly recovered most of its original shape without external resistance (**Fig. S6**). The incomplete shape recovery is due to the release of physically absorbed water in the gel network under large deformation, which in turn demonstrates the high water content (~90%) in the gel. This fast recovery behavior is attributed to the phase-separated domains in the PSG that serve as crosslinkers to strengthen the hydrogel network and dissipate energy.

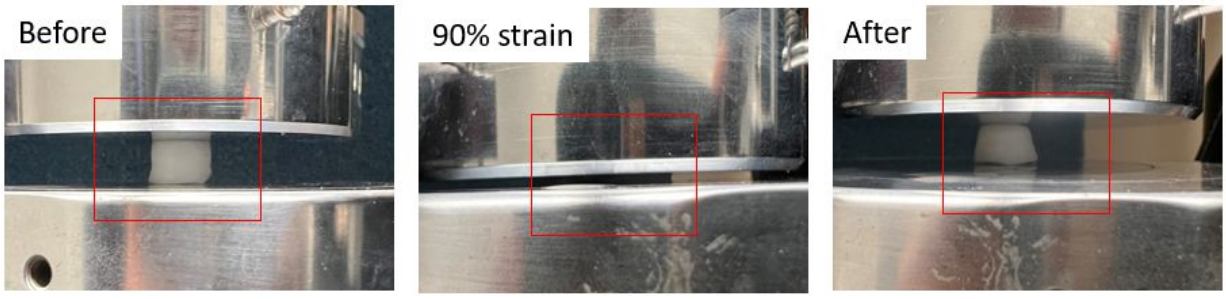

Fig. S6. Photographs of PSG during extreme compression.

As shown in **Fig. S7a**, the PSG immersed in 4 M NaCl solution gives the largest stress of 1.5 MPa as the hydrogel was stretched to 350%. Additionally, ion diffusion within the network contributed to the modulation of the gel's ionic conductivity (**Fig. S7b**). The ionic conductivity of the PSG increased from 1×10^{-3} mS cm^{-1} to 4 $\times10^{-3}$ mS cm^{-1} when immersed in 1 M NaCl due to the diffusion of Na^+ and Cl^- ions into the pores of the PSG (**Fig. S7b**). Ionic conductivity decreased to ~2×10^{-3} mS cm^{-1} upon continued salt addition. This may be attributed to the salting out effect induced by crosslinking in the PSG, leading to a denser and more rigid structure that hindered the movement of ions.

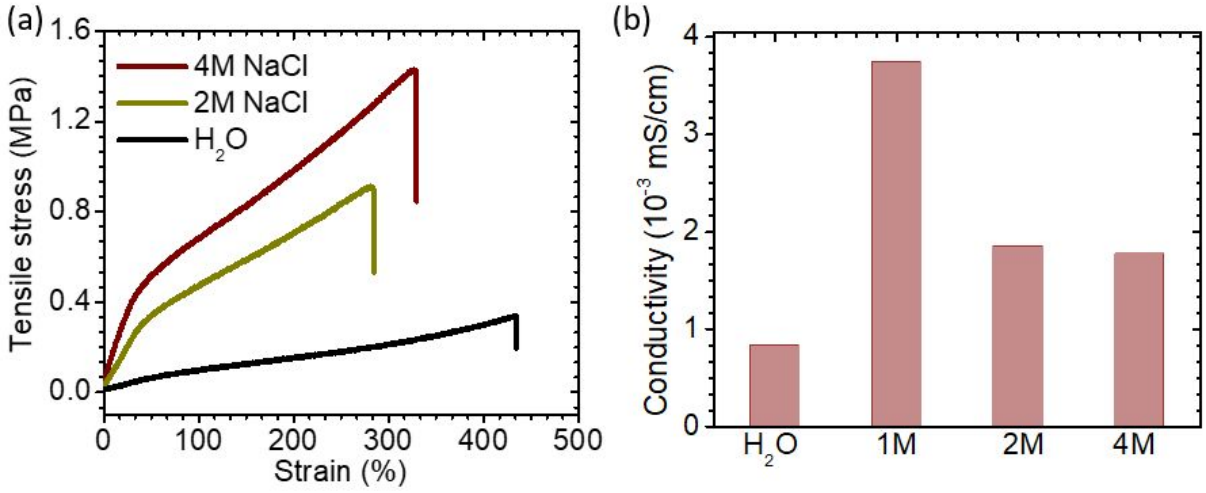

Fig. S7. The stress-strain curves (a) and conductivity (b) of a PSG after immersion into different NaCl concentrated solutions.

Covalent hydrogels are disposable and non-recyclable because of permanent covalent crosslinks, which prevent reuse and reprocessing. In our work, the PSG is crosslinked by non-covalent supramolecular interactions, which allows for the recycling of the gel. As shown in **Fig. S8**, upon heating at an elevated temperature (80 °C), the hydrogen bonds and hydrophobic interactions within the PSG were disrupted. As a result, the PSG melted and formed a translucent liquid. The liquid is viscous due to the electrostatic interactions between the polymer chains. The viscosity rise upon cooling to room temperature suggests the formation of new molecular interactions. Finally, the viscous solution was reformed into gels of various shapes using the dehydration-hydration method. The phase-separated domains and the continuous porous structure were retained in the reprocessed gel.

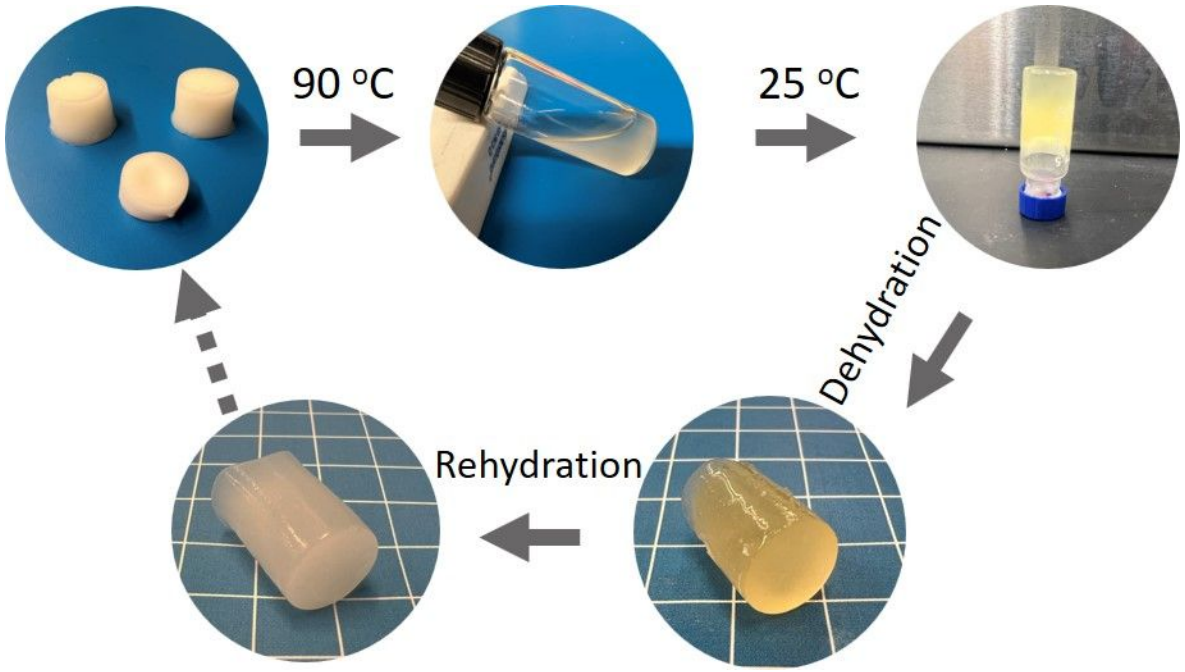

Fig. S8. Recycling and reprocessing of PSG.

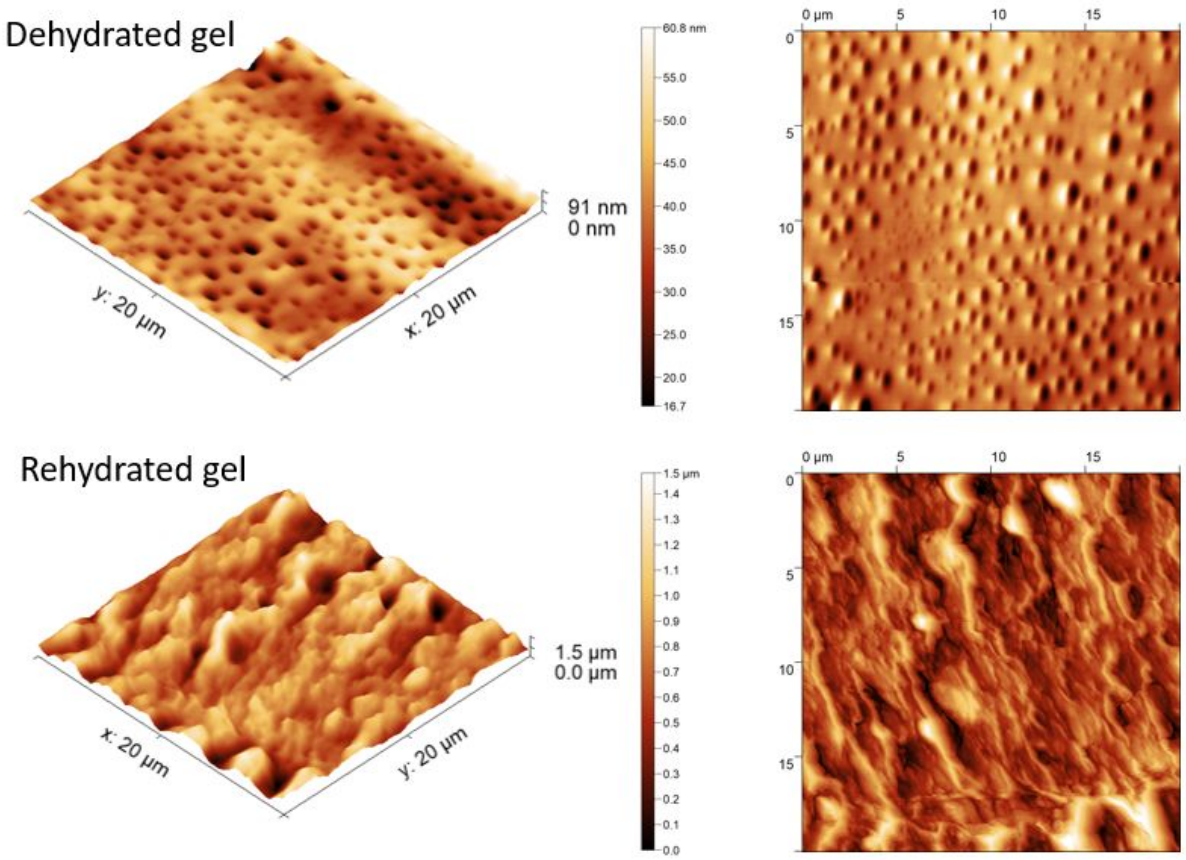

Fig. S9. AFM of dehydrated SG and the PSG after rehydration.

The as-prepared SG hydrogels with varied monomer ratios were directly submerged in water for hydration. The soft and stretchable SGs tended to absorb water and swell when placed in an aqueous environment, thus significantly decreasing mechanical properties. As shown in **Fig. S10**, the SG with a monomer ratio of 100:0 eventually dissolved in water over time. The softening and dissolution of supramolecular hydrogels is a thermodynamically favorable process due to a gain in the entropy of the overall system.[5] The dehydration-hydration approach used to form PSGs is necessary to achieve a tough hydrogel.

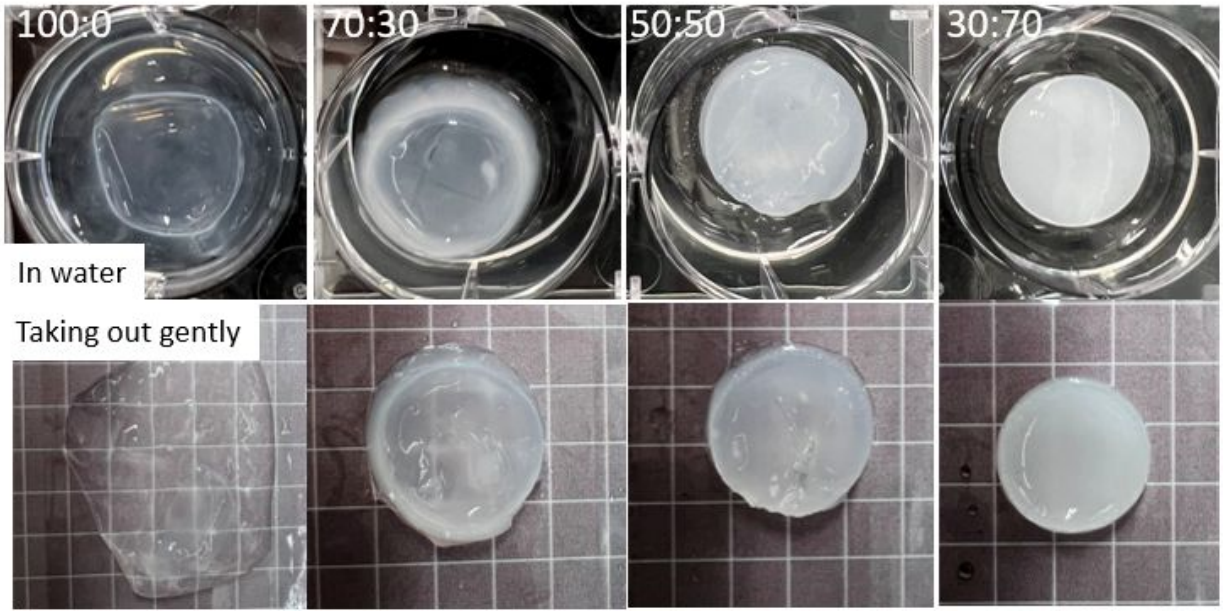

Fig. S10. Swelling behavior of SGs in distilled water.

As shown in **Fig. S11a**, the PSG with NaSS and SBMA monomer absorbed water and reached an equilibrium swollen state within one day. The equilibrium state was stable for at least ten days. In contrast, the swelling ratio of the PSG without SBMA increased up to a maximum value within one day, after which it started to decrease until achieving a stable equilibrium swollen state. This swelling-to-deswelling behavior is due to the decreased osmotic pressure *via* extraction of free copolymer chains during swelling to the surrounding environment. In the swollen equilibrium state, the PSG with various monomer ratios showed an opaque color, and the water content approached ~ 90 wt%.

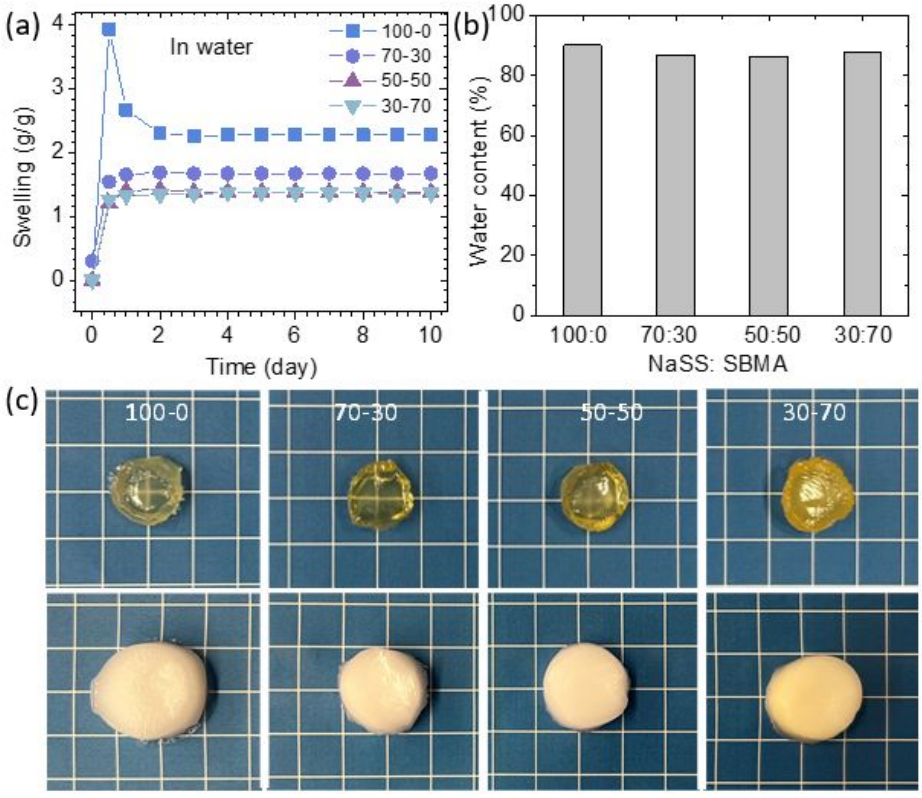

Fig. S11. (a) Swelling kinetics of PSG with various monomer ratios in water. (b) Equilibrium water content in swollen PSG with various monomer ratios and (c) the corresponding volume changes.

The stability of PSG at different pH and in seawater was also recorded (**Fig. S12a-d**). The PSG without SBMA monomer exhibited a pH-dependent swelling behavior because of the pH-sensitive -SO_3^- groups. For the PSGs, there were no major differences in the swelling ratio in the solutions. This comparison indicates the critical role of SBMA in keeping the network stable in various environmental conditions.

When exposed to seawater, the osmotic pressure difference between the gel and the environment decreased due to the presence of corresponding ions, resulting in a reduced swelling ratio. In the case of salt water, the Hofmeister effect causes PVA chains to form a crystalline structure, thus increasing the physical crosslinking of the network and inhibiting water absorption. On the other hand, the gel's zwitterionic component promotes water penetration by disrupting electrostatic interactions between -N+(CH3)3 and -SO3- groups. As a result, PSG can still swell to some extent in concentrated salt water.

The environment-tolerance characteristic of PSG provides a significant advantage over covalently crosslinked hydrogels and non-covalent supramolecular hydrogels. It indicates that phase-separated domains in PSG can stabilize and strengthen supramolecular bonds in a wet environment. **Fig. S13** shows the swelling behavior of PSG in various solvents.

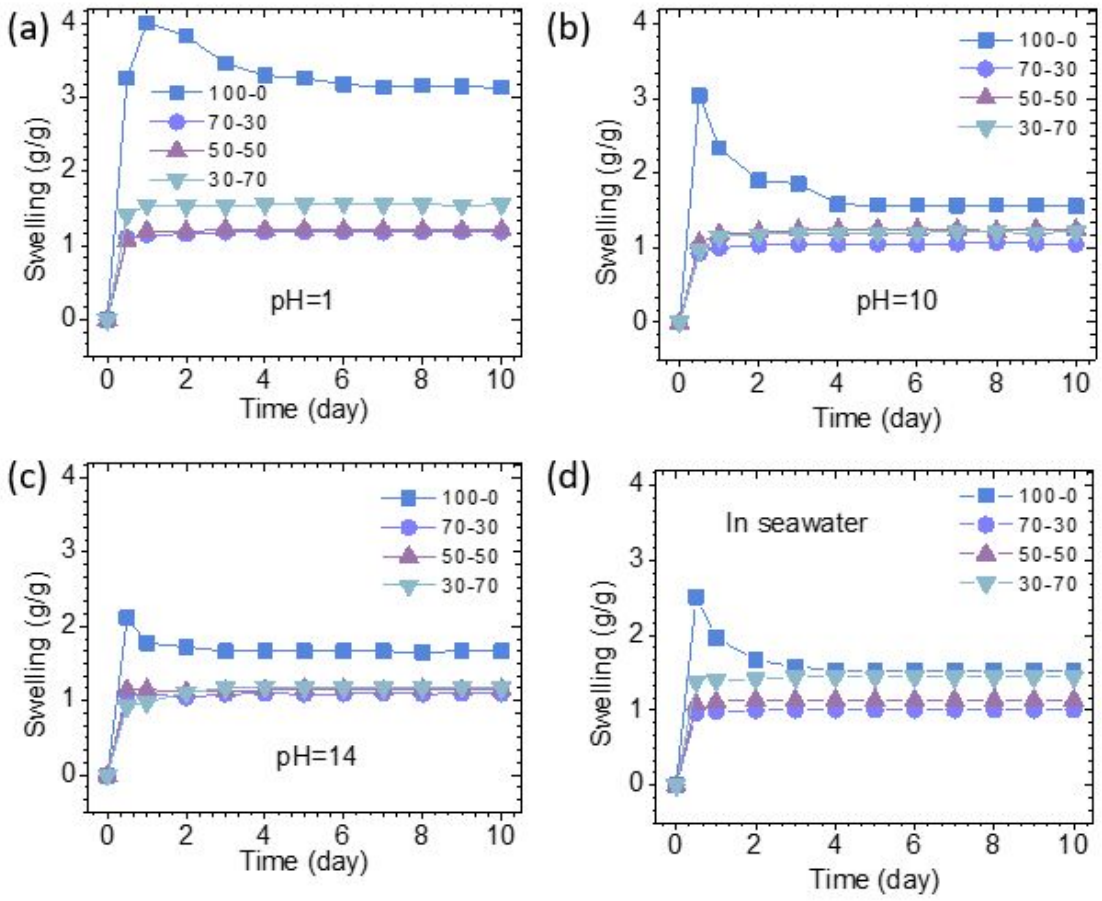

Fig. S12. Swelling kinetics of PSG with different monomer ratio aqueous solution with varied pH (a-c) and in seawater (d).

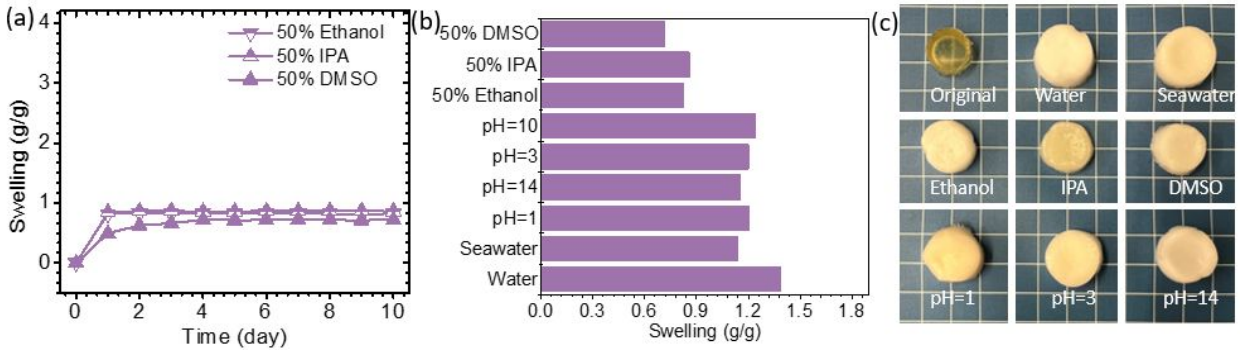

Fig. S13. (a) Swelling kinetics of PSG with monomer ratio of 50:50 in mixed solvents. (b) Equilibrium swelling ratio of PSG in various liquids. (c) Photographs of swollen PSG in various liquids.

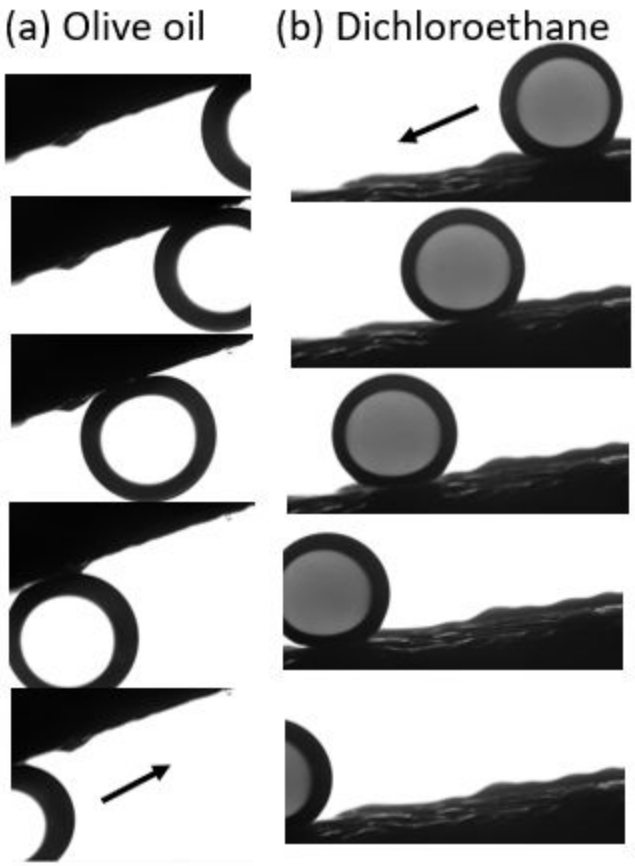

Fig. S14. (a) The underwater sliding behavior of (b) olive oil and (b) 1,2-dichloroethane droplets atop PSG.

Colloid probe force microscopy was further employed to quantify the underwater oil adhesion force on the surface of PSG, as shown in **Fig. S15a, b**. A soft polyethylene colloidal probe was used as a model oil foulant to contact the hydrogel surface.[1] Adhesion forces were very small (less than one μN) associated with the superhydrophilicity of the hydrogel surface. This anti-oil adhesion was confirmed by continuously placing dye-labeled 1,2-dichloroethane onto the PSG surface in an aqueous environment. As shown in **Fig. S15c**, a jet of 1,2-dichloroethane spontaneously bounces off the surface without leaving any visible oil residue, further demonstrating the excellent oil resistance of the PSG. Furthermore, after being submerged in olive oil, the surface of PSG is slightly wetted by olive oil in an air environment. The attached olive oil completely detached from the PSG surface by washing with water only (**Fig. S15d**). These results imply that PSG was thoroughly cleaned without the need for energy- or chemical-intensive surface cleaning processes. These findings demonstrate the goals of the design philosophy, incorporating a zwitterionic component into the PSG to create an antifouling hydrogel that prevents surface contamination. The anti-oil fouling and self-cleaning properties can be explained as follows[6]: the zwitterionic component of PSG has a strong water affinity and generates a hydration water layer around the gel surface.

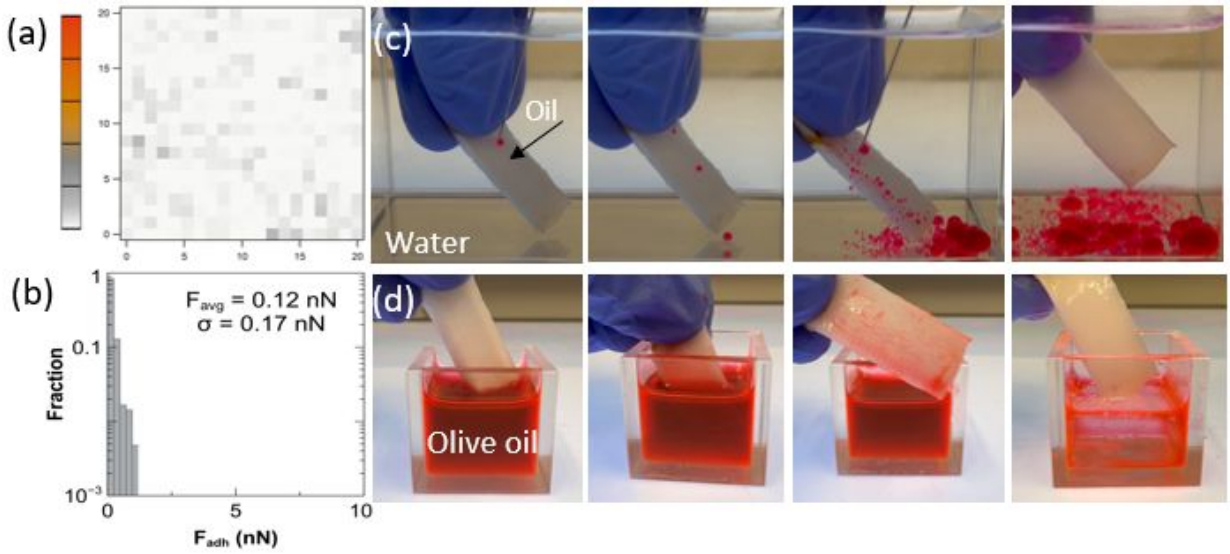

Fig. S15. Colloid probe force microscopy measurement of adhesion force map (a) and histogram with average adhesion force and variance (σ) (b). Photos of Nile red-labeled 1,2-dichloroethane

sliding down a tilted PSG surface in water (c). Photos of the PSG contaminated by the Nile red-labeled olive oil before and after being washed by water (d).

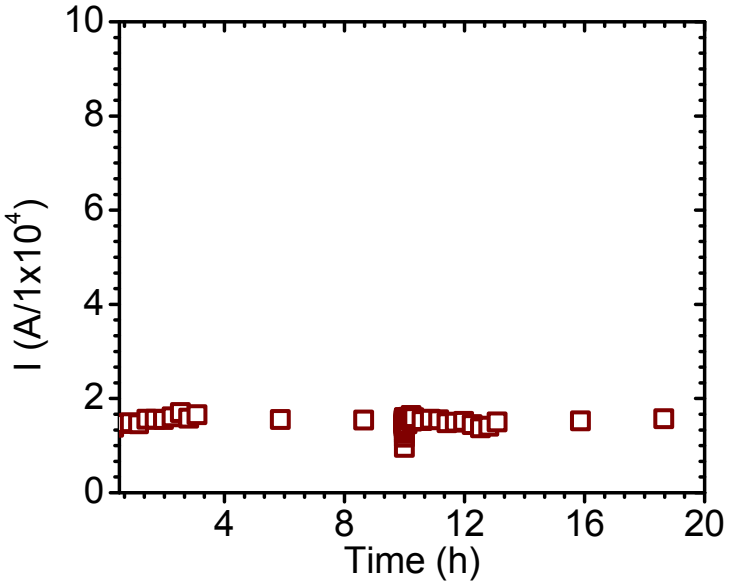

Fig. S16. Chronoamperometry measurement of PSG held for 20 hours at 1000 mV.

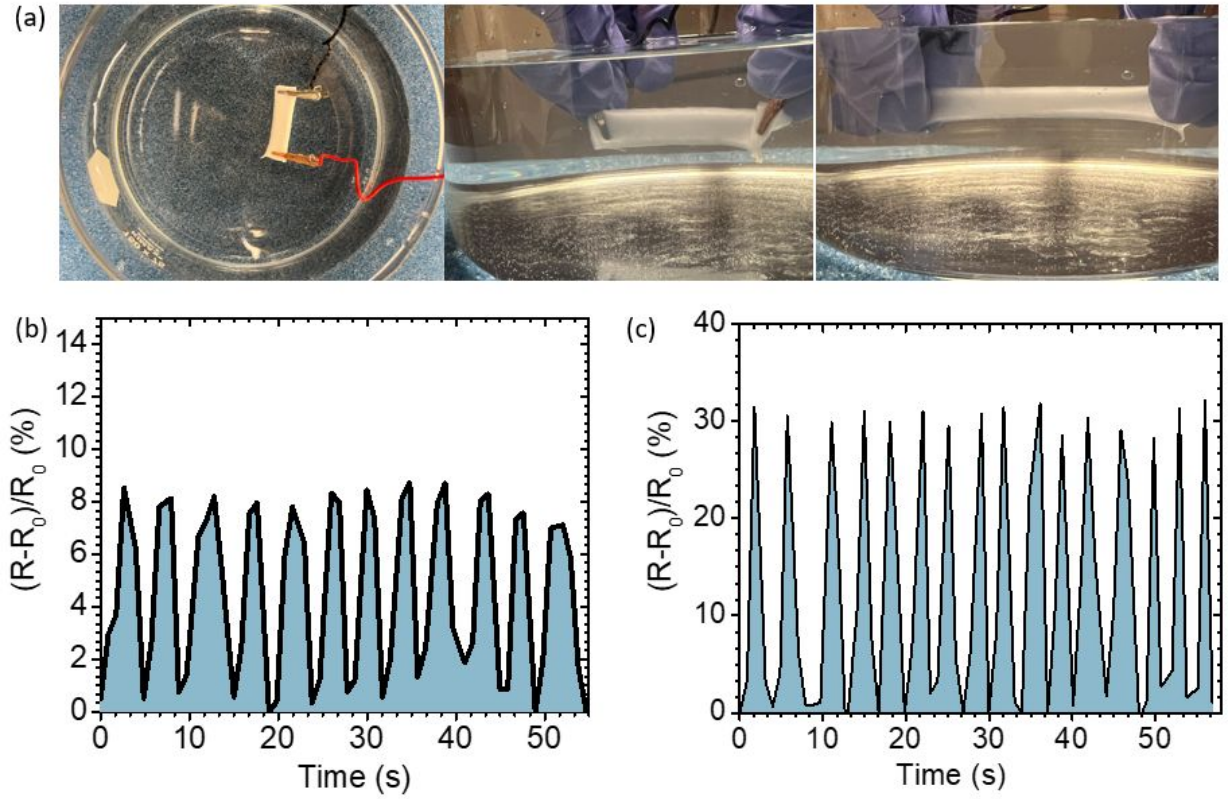

Fig. S17. (a) Underwater stretching of PSG for measuring resistance changes. Relative resistance changes of the PSG in an underwater environment at (b) 20% strain and (c) 50% strain.

References

1 Horseman, T., Wang, Z. & Lin, S. Colloidal interactions between model foulants and engineered surfaces: Interplay between roughness and surface energy. *Chemical Engineering Journal Advances* **8**, 100138 (2021).

2 Davenport, D. M., Lee, J. & Elimelech, M. Efficacy of antifouling modification of ultrafiltration membranes by grafting zwitterionic polymer brushes. *Separation and Purification Technology* **189**, 389-398 (2017).

3 Liu, C., Lee, J., Ma, J. & Elimelech, M. Antifouling thin-film composite membranes by controlled architecture of zwitterionic polymer brush layer. *Environmental science & technology* **51**, 2161-2169 (2017).

4 Liu, C., Lee, J., Small, C., Ma, J. & Elimelech, M. Comparison of organic fouling resistance of thin-film composite membranes modified by hydrophilic silica nanoparticles and zwitterionic polymer brushes. *Journal of Membrane Science* **544**, 135-142 (2017).

5 Draper, E. R. & Adams, D. J. Low-molecular-weight gels: the state of the art. *Chem* **3**, 390-410 (2017).

6 Schlenoff, J. B. Zwitteration: coating surfaces with zwitterionic functionality to reduce nonspecific adsorption. *Langmuir* **30**, 9625-9636 (2014).